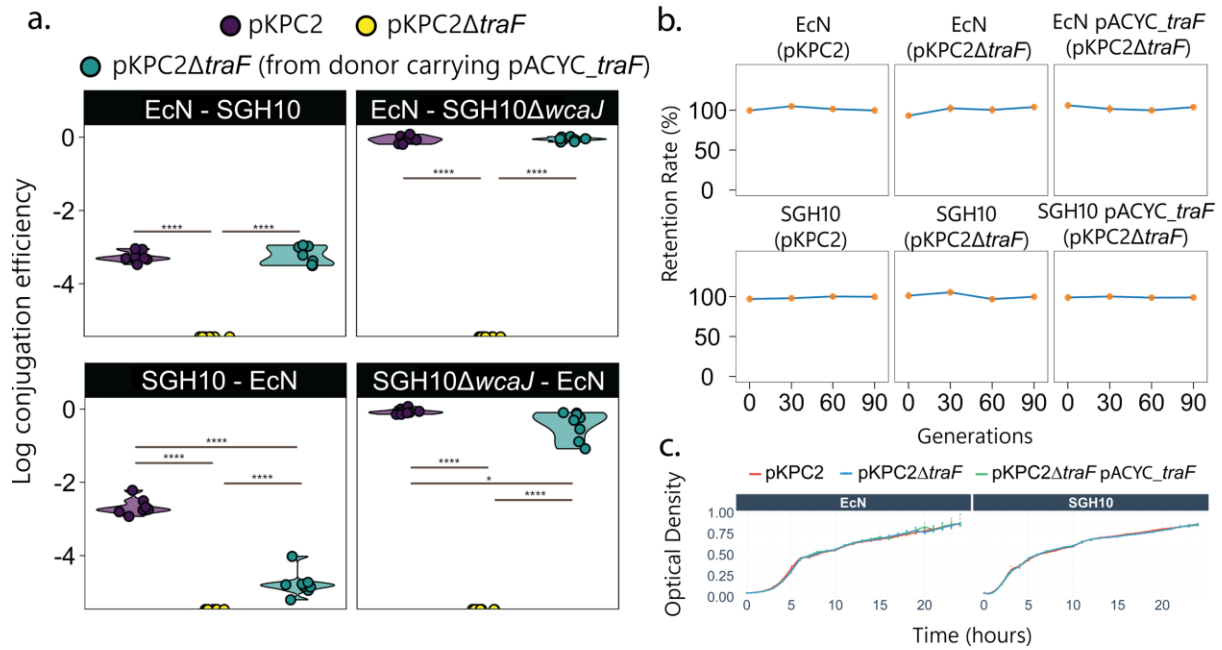
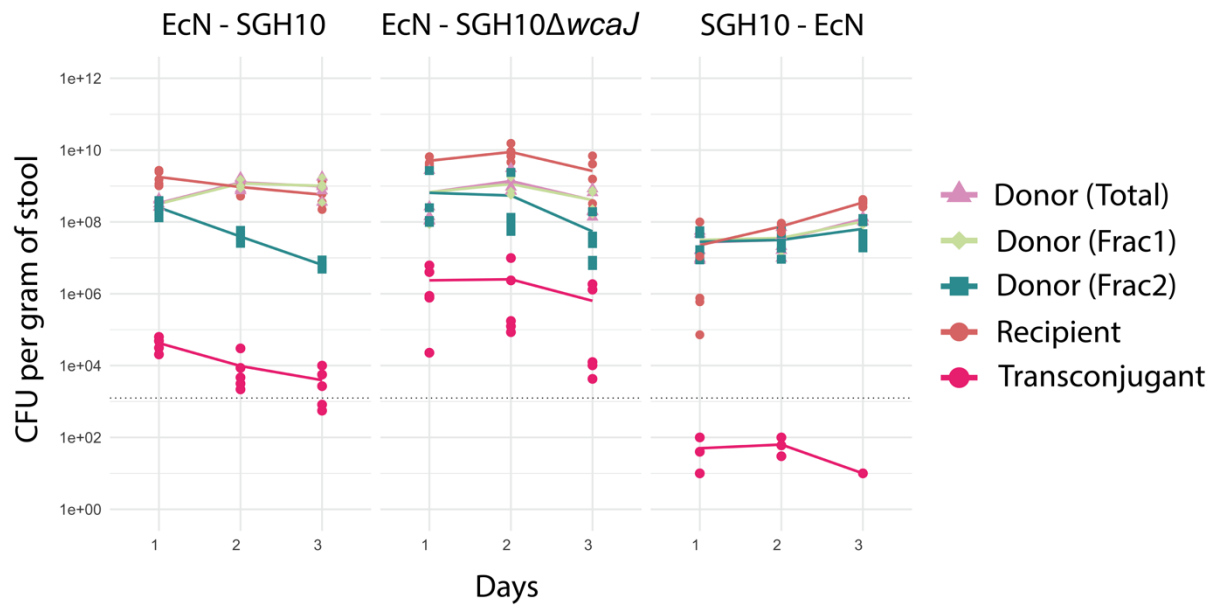


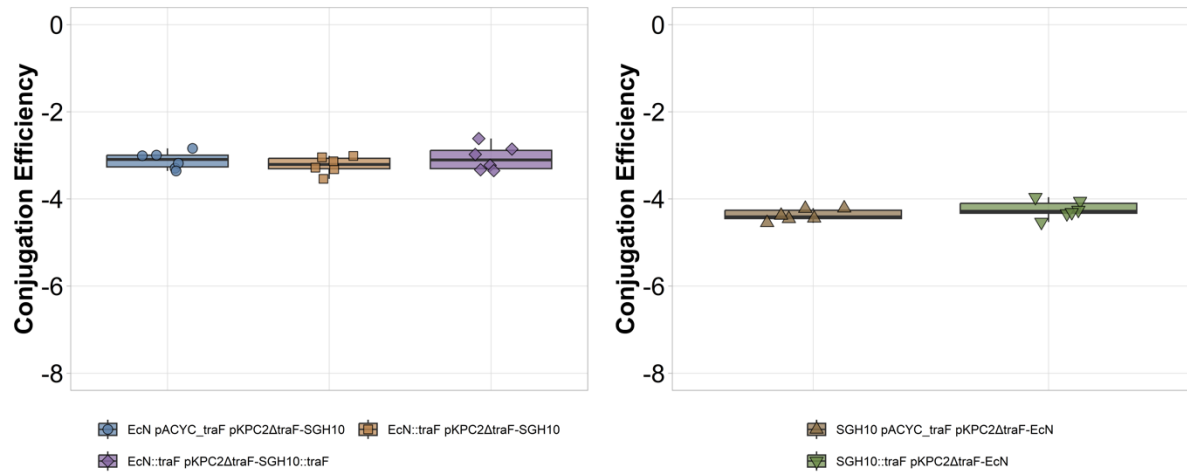
**Supplementary Fig. 1: Growth kinetics of EcN, SGH10 and SGH10 $\Delta wcaJ$  in LB carrying different plasmids.** Growth curve showing the optical density (OD<sub>600</sub>) of EcN, SGH10 and SGH10 $\Delta wcaJ$  with or without the respective plasmids in LB over 24 hours. Each timepoint included four biological replicates. The statistical differences between the plasmid groups were analyzed by first calculating the area under the curve for each group. One-way ANOVA (Dunnett's test) was then conducted to compare the plasmid-bearing groups with the plasmid-free control. Statistically significant differences were indicated on the graph, with the corresponding p-values displayed.



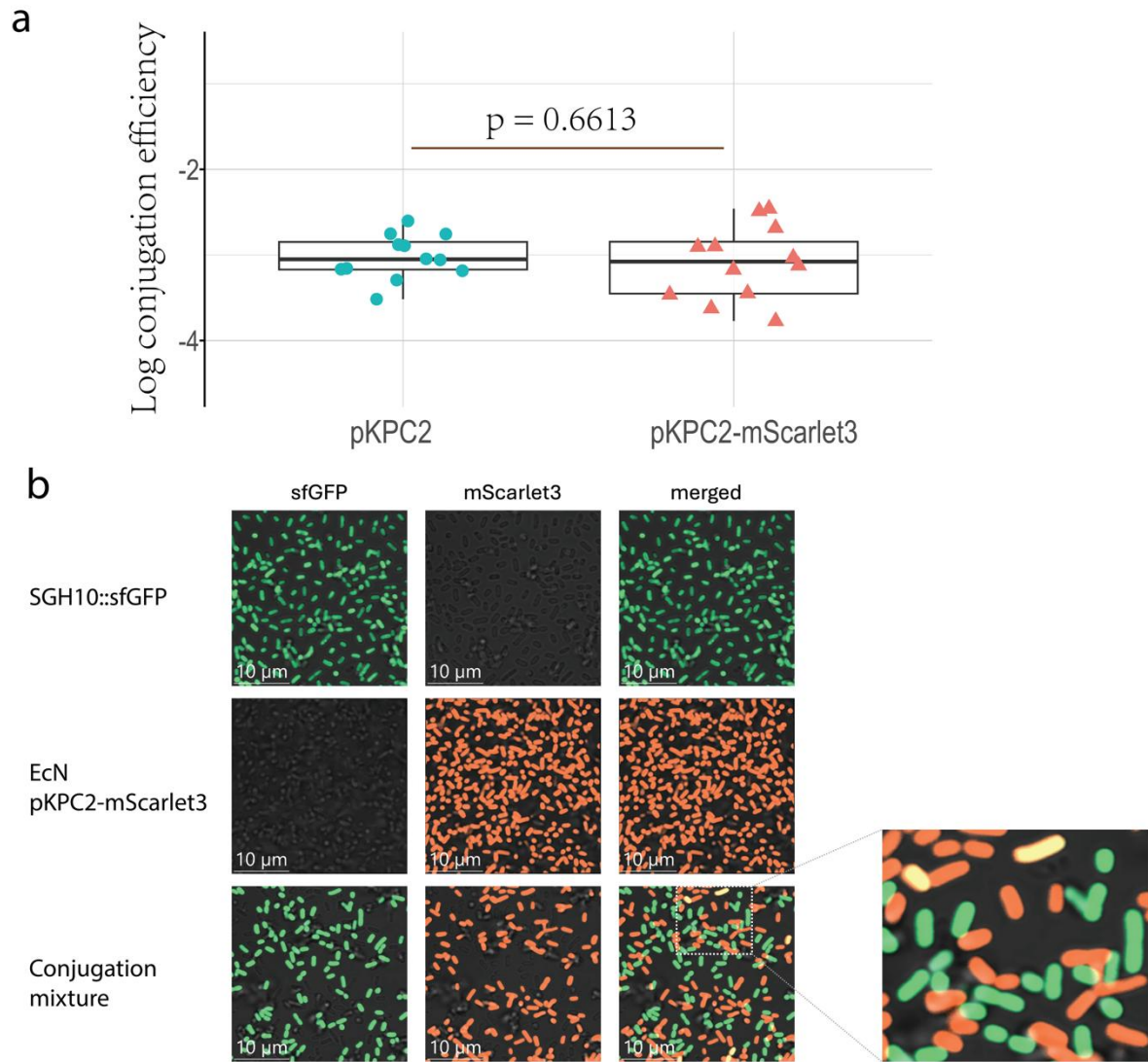
**Supplementary Fig. 2: *In vitro* characterisation of pKPC2ΔtraF.** (a) Violin plot of log<sub>10</sub>-transformed conjugation efficiency for four donor-recipient pairs: EcN-SGH10, EcN-SGH10ΔwcaJ, SGH10-EcN, and SGH10ΔwcaJ-EcN, using plasmids pKPC2, pKPC2ΔtraF (unable to conjugate due to the lack of an essential transfer gene), and pKPC2ΔtraF with EcN donor complemented with a non-mobilizable plasmid carrying *traF* (pACYC\_traF) in trans, allowing only primary transfer from donor to recipient. Each dot represents a biological replicate (n=8 per group) from three independent experiments. Statistical differences were assessed using one-way ANOVA (Tukey's correction), with significant differences indicated by asterisks. The exact p-values (pKPC2 vs. pKPC2ΔtraF, pKPC2 vs. pKPC2ΔtraF pACYC\_traF, pKPC2ΔtraF vs. pKPC2ΔtraF pACYC\_traF): EcN-SGH10 (<0.0001, 0.9821, <0.0001); EcN-SGH10ΔwcaJ (<0.0001, 0.9074, <0.0001); SGH10-EcN (<0.0001, <0.0001, <0.0001); SGH10ΔwcaJ-EcN (<0.0001, 0.0102, <0.0001). (b) Plasmid stability of the mutant plasmid in EcN or SGH10, with or without the complementation plasmid pACYC\_traF. The dot represents the mean value of six biological replicates from three independent experiments. (c) Growth curve showing the optical density (OD<sub>600</sub>) of EcN and SGH10 carrying pKPC2, pKPC2 ΔtraF or pACYC\_traF pKPC2ΔtraF grown in LB over 24 hours. Statistical differences were compared against a reference group pKPC2 and analyzed by one-way ANOVA (Dunnnett's test) based on the area under the curve for each group (n=6 biological replicates per group), and no significant differences were observed. The exact p-values: EcN pKPC2ΔtraF vs. EcN pKPC2 (0.9275); EcN pKPC2ΔtraF pACYC\_traF vs. EcN pKPC2 (0.4699); SGH10 pKPC2ΔtraF vs. SGH10 pKPC2 (0.0664); SGH10 pKPC2ΔtraF pACYC\_traF vs. SGH10 pKPC2 (0.1665).



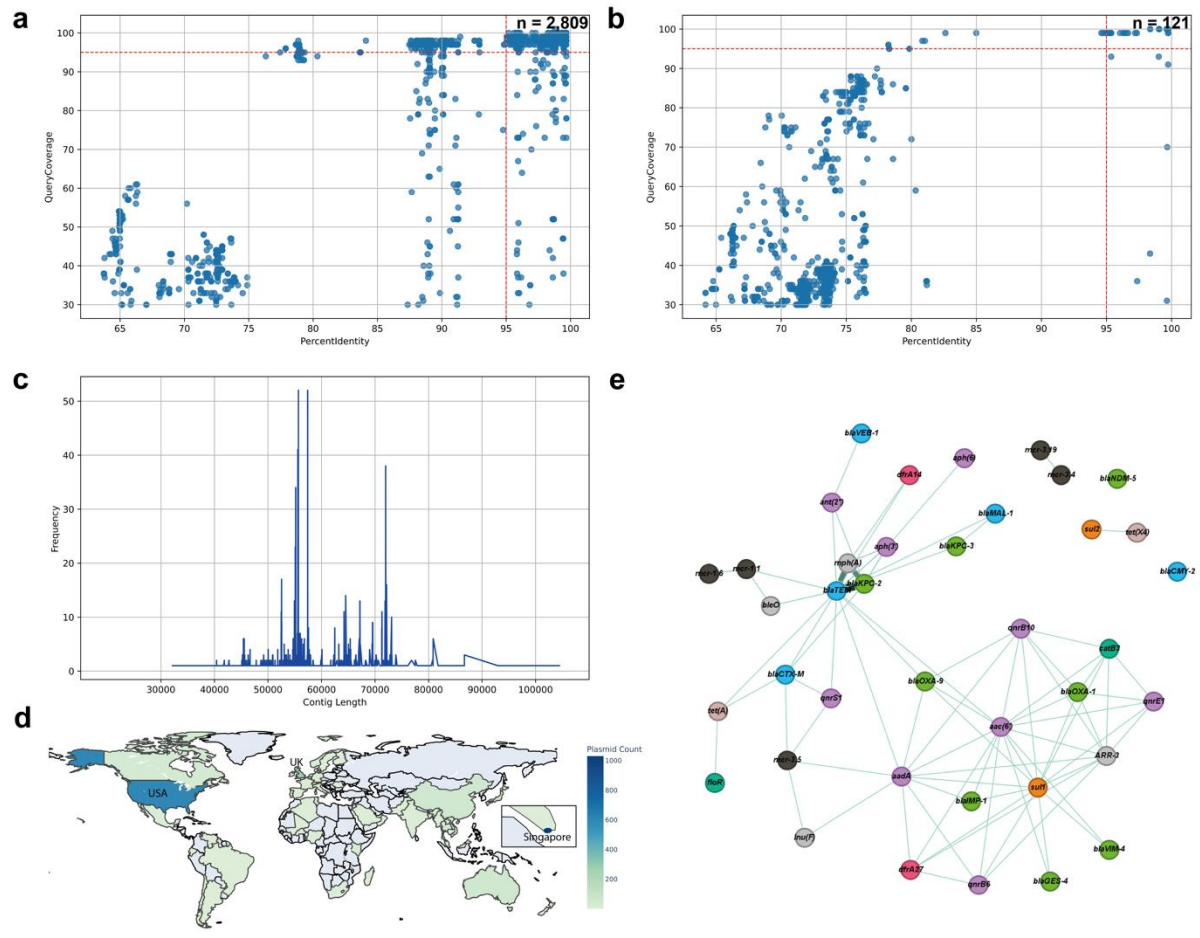
**Supplementary Fig 3: Counts of recipient, donor and transconjugant for the primary transfer of pKPC2ΔtraF *in vivo*.** The recipient, donor (total donor count), donor (frac1 = the fraction of donors harbouring pKPC2ΔtraF), donor (frac2 = the fraction of donors harbouring both pKPC2ΔtraF and pACYC\_traF) and transconjugant on days 1, 2, and 3 were measured from stools of five mice per group. The counts are expressed as CFU per gram of stool. The dotted line represents limit of detection.



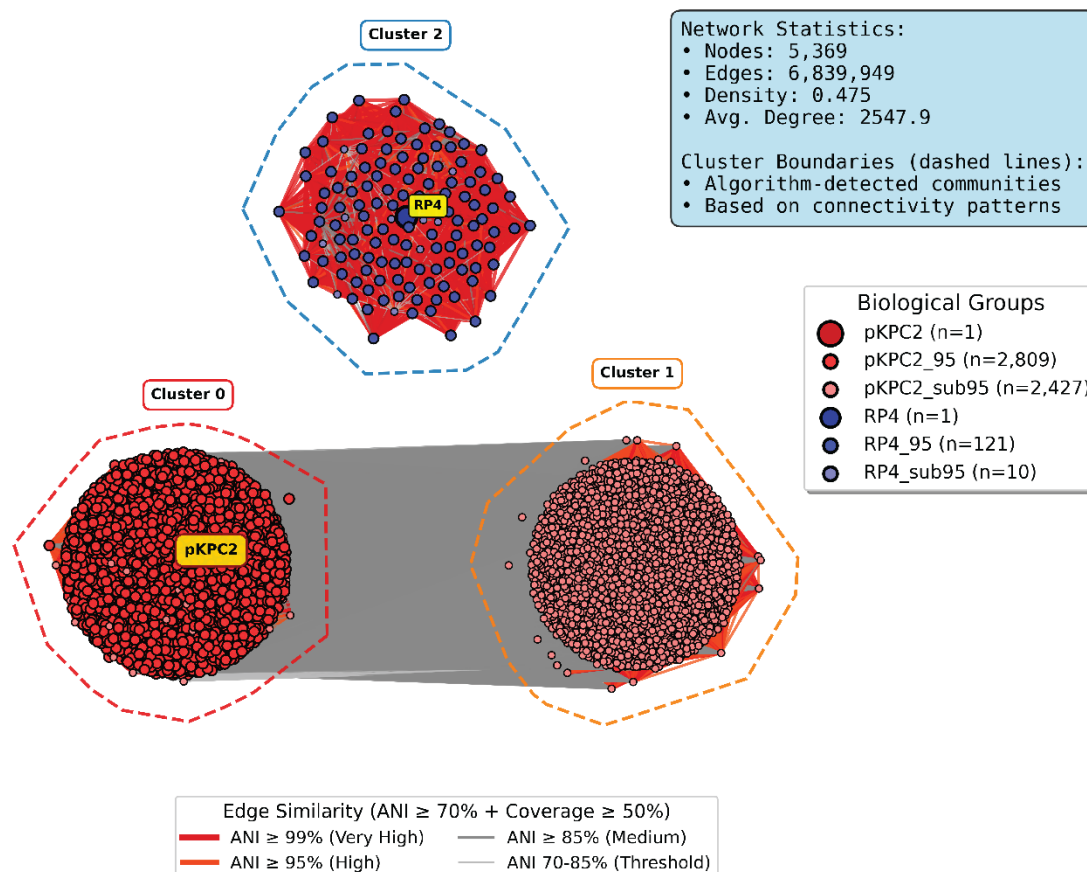
**Supplementary Fig 4: *In vitro* conjugation of pKPC2ΔtraF into SGH10::traF.** Log<sub>10</sub>-transformed *in vitro* conjugation efficiency of pKPC2ΔtraF from EcN pACYC\_traF pKPC2ΔtraF to SGH10, EcN::traF pKPC2ΔtraF to SGH10 or SGH10::traF, and SGH10 pACYC\_traF pKPC2ΔtraF or SGH10::traF pKPC2ΔtraF to EcN. The centre line of the boxplot denotes the median, the box bounds indicate the 25<sup>th</sup> and 75<sup>th</sup> percentiles, and the whiskers extend to 1.5X the IQR. Data represent six biological replicates from three independent experiments. Statistical analysis was performed using one-way ANOVA (Tukey's multiple comparisons test) for the three groups with EcN as donors and unpaired t-test with Welch's correction (two-sided) for the two groups with SGH10 as donors. No significant difference was identified. The exact p-values: EcN::traF pKPC2ΔtraF-SGH10 vs. EcN::traF pKPC2ΔtraF-SGH10::traF (0.4747); EcN::traF pKPC2ΔtraF-SGH10 vs. EcN pACYC\_traF pKPC2ΔtraF-SGH10 (0.7031); EcN::traF pKPC2ΔtraF -SGH10::traF vs. EcN pACYC\_traF pKPC2ΔtraF-SGH10 (0.9222); SGH10 pACYC\_traF pKPC2ΔtraF-EcN vs. SGH10::traF pKPC2ΔtraF-EcN (0.2148).



**Supplementary Fig. 5: Conjugation of pKPC2-mScarlet3 *in vitro*.** (a) Log<sub>10</sub>-transformed conjugation efficiency of pKPC2 (●) from EcN KN02 to SGH10 and pKPC2-mScarlet3 (▲) from EcN KN03 to SGH10::sfGFP. The centre line of the boxplot denotes the median, the box bounds indicate the 25<sup>th</sup> and 75<sup>th</sup> percentiles, and the whiskers extend to 1.5X the IQR. Statistical differences of n=12 biological replicates per group from three independent experiments were determined using unpaired t test with Welch's correction (two-sided). The exact p-value is shown on the graph. (b) Confocal microscopy images of SGH10::sfGFP alone, EcN KN03 pKPC2-mScarlet alone and the conjugation mixture of both strains. The zoom-in image shows the yellow color in the cells indicating the presence of transconjugants. These images were taken using Olympus FV3000 confocal laser scanning microscope at 100X. Images shown are representative images of three biological replicates and all replicates showed consistent results.



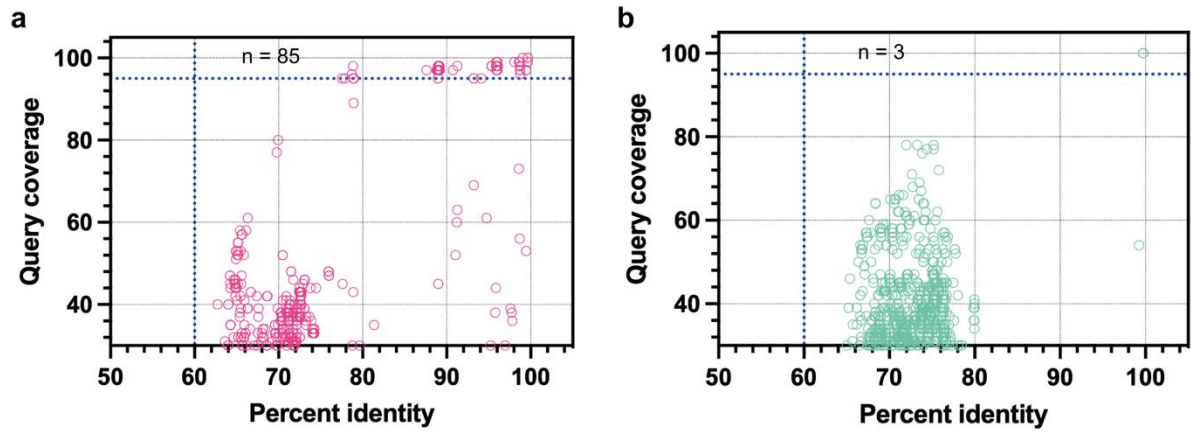
**Supplementary Fig. 6: pKPC2-like sequences in ENA database.** (a) Distribution of pKPC2-like sequences and (b) RP4-like sequences, with 2,809 and 121 sequences, respectively, meeting the 95% nucleotide identity and coverage thresholds for pKPC2 and RP4. These results are based on BlastN analysis, using 22 conserved T4SS genes and the *trfA* gene as query sequences. (c) Contig length distribution for pKPC2-like sequences. (d) Geographical distribution of pKPC2-like sequences, showing that the majority originated from Singapore, the USA, and the UK. The map was created using the Plotly package in Python. (e) The carriage of ARGs on pKPC2-like sequences, where each node represents a specific ARG, and edges between nodes indicate that the pair of ARGs co-occur on the same contig. The thickness of each edge corresponds to the frequency of co-occurrence, with thicker edges indicating more frequent associations (e.g., *blaTEM* and *blaKPC-2* are the most commonly co-carried ARGs in pKPC2-like sequences). The network graph was created on Gephi 0.10.



**Supplementary Fig. 7: Network analysis of plasmid similarity based on Average Nucleotide Identity (ANI).**

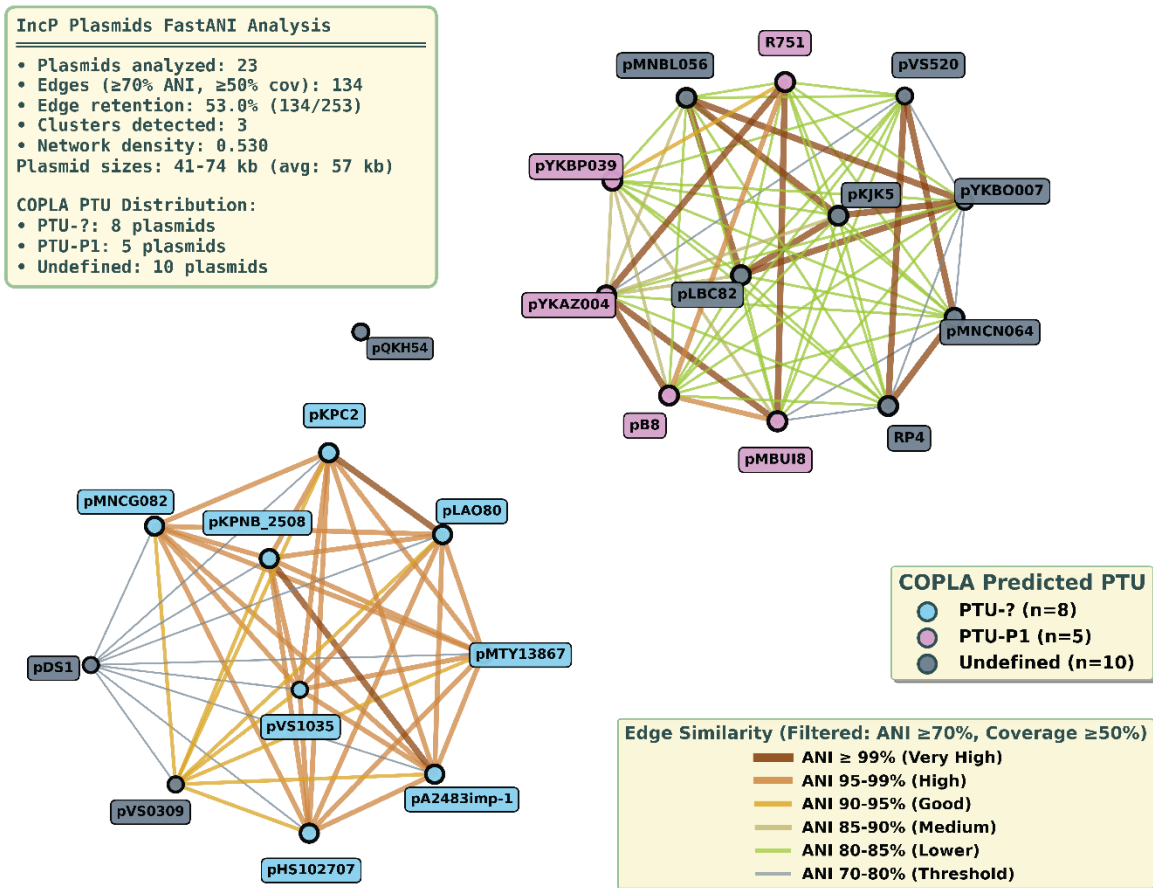
Each node represents a plasmid sequence: pKPC2 (reference), pKPC2\_95 (pKPC2-like sequences with  $\geq 95\%$  nucleotide identity and query coverage to the pKPC2 T4SS and replicon), pKPC2\_sub95 (pKPC2-like sequences with  $\geq 80\%$  but  $< 95\%$  identity/coverage), RP4 (reference), and its RP4\_95 and RP4\_sub95 groups. Nodes are colored according to plasmid type: pKPC2-like (red/pink) or RP4-like (blue). Edges represent similarity relationships (ANI  $\geq 70\%$ , coverage  $\geq 50\%$ ), with edge width and color reflecting similarity strength (thicker, darker red edges = ANI  $\geq 95\%$ ; thinner grey edges = lower similarity above threshold). Dashed boundaries indicate clusters identified by network connectivity. The network shows distinct, non-interconnected clusters for pKPC2-like and RP4-like sequences. Within the pKPC2-like group, two sub-clusters are observed, with inter-cluster connections primarily in grey (lower ANI) and intra-cluster connections in red (higher ANI).



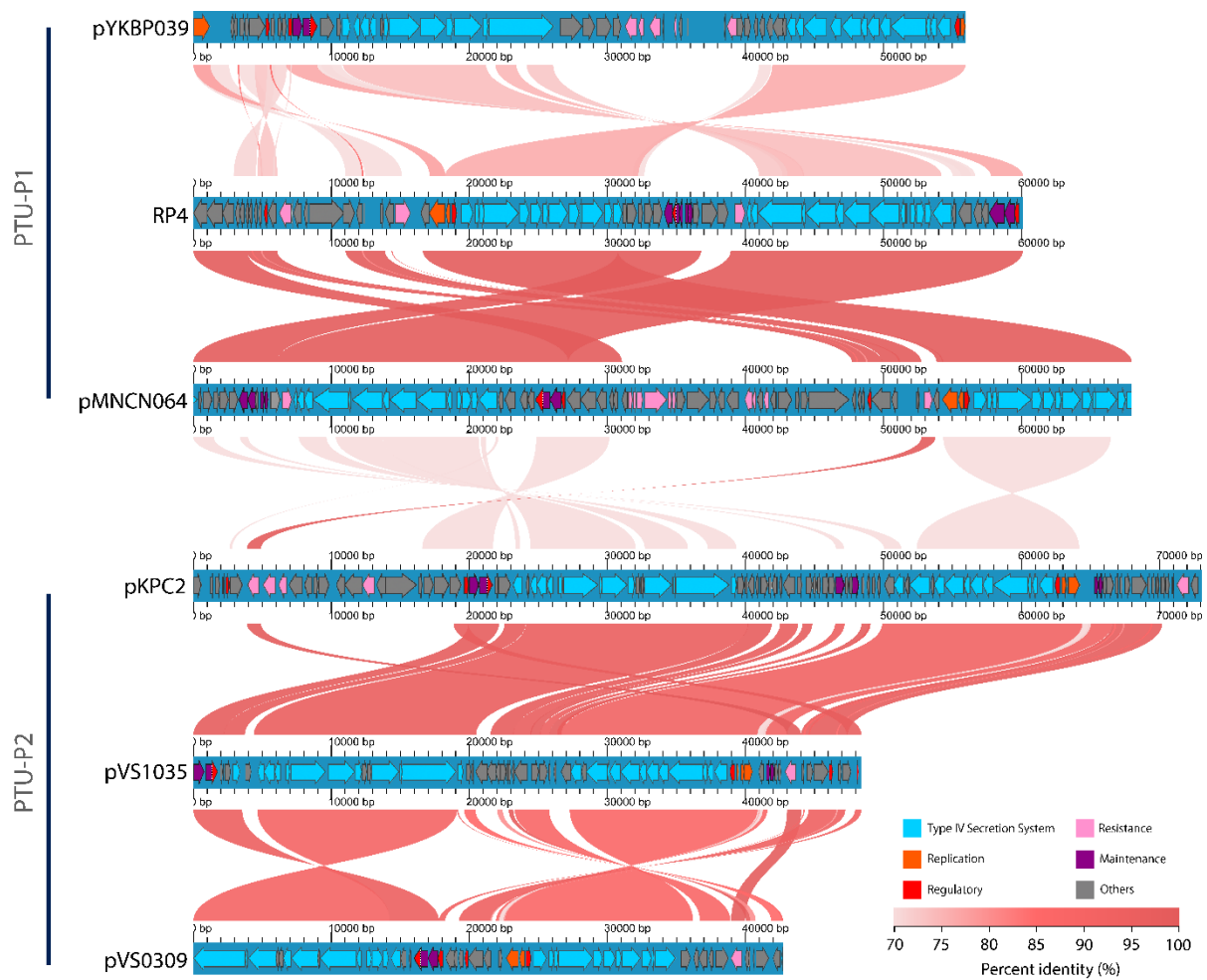


**Supplementary Fig. 8: Prevalence of pKPC2-like and RP4-like plasmids in IMG/PR database.** (A) Distribution of pKPC2-like plasmids, with 85 plasmids meeting the 95% query coverage and 60% nucleotide identity criteria. (B) Distribution of RP4-like plasmids, with only 3 plasmids matching the same 95% query coverage and 60% nucleotide identity threshold. These results are based on BlastN analysis, using 22 conserved T4SS genes and the *trfA* gene as query sequences.

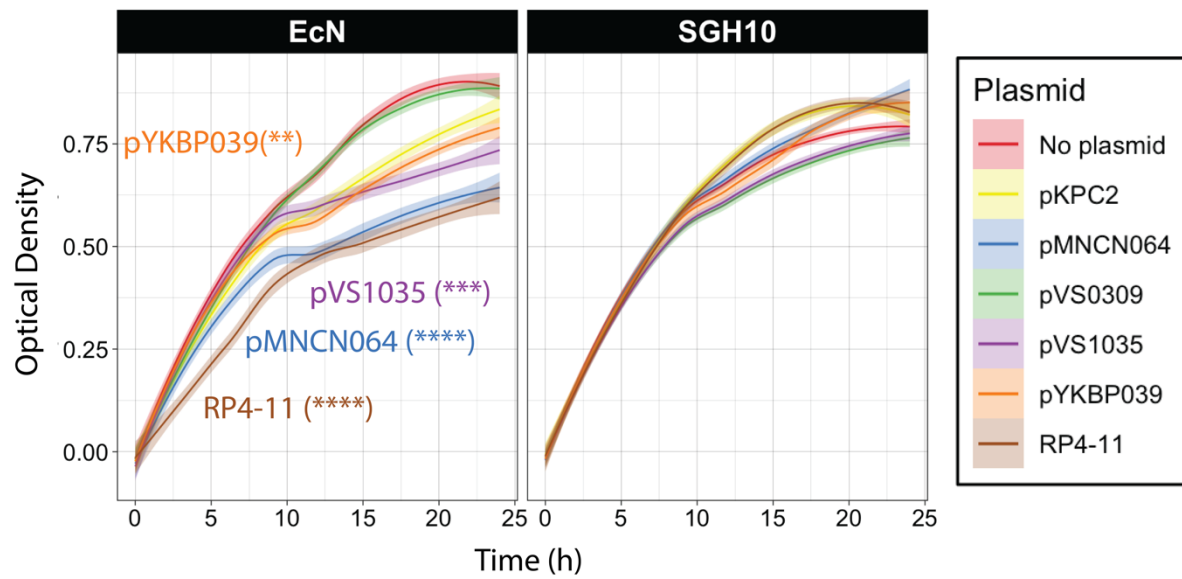




**Supplementary Fig. 9: Network analysis of IncP clade I and II plasmids with COPLA assignment.** Pairwise comparisons of clade I and II plasmids were performed using FastANI to calculate average nucleotide identity (ANI), which was then used for Louvain clustering. Each node represents a plasmid, with node color indicating COPLA-based PTU assignment (blue = PTU-?, pink = PTU-P1, grey = undefined). Edges represent similarity relationships (ANI  $\geq 70\%$ , coverage  $\geq 50\%$ ), with edge thickness proportional to ANI strength (thicker edges = higher ANI values).



**Supplementary Fig. 10: Plasmid alignment map.** The entire plasmid sequences of PTU-P1 plasmids (RP4, pMNCN064, pYKBP039) and PTU-P2 plasmids (pKPC2, pVS0309, pVS1035) were aligned using the Alignment Toolbox and Visualization (AliTV). A red gradient ribbon links pairs of plasmids, representing aligned regions with shading that reflects percent identity. Genes on each plasmid are color-coded by functional categories: type IV secretion system, regulatory, resistance (antibiotic and heavy metal), replication, maintenance, and other genes not belonging to those categories. One gene, *korB*, is known for its dual function in regulation and maintenance. Thus, it is color-coded with one half in red and the other half in purple.



**Supplementary Fig. 11: Growth curve of EcN and SGH10 in LB carrying PTU-P1 or PTU-P2 plasmids.** Growth curves of EcN and SGH10 with and without plasmids over 24 hours in LB. Each timepoint included 18 biological replicates from three independent experiments. Statistical analysis was performed using the area under the curve, followed by one-way ANOVA (Dunnett's test) to compare plasmid-bearing strains with plasmid-free control as reference group. Only p-values less than 0.05 are displayed on the graph. The results shown are representative of three independent experiments.

**Supplementary Table 1. Bacterial strains and plasmids used.**

Strains	Features	Reference
<i>K. pneumoniae</i>		
SGH10	hvKp KL1, ST23; Fm <sup>R</sup>	1
SGH10::sfGFP	SGH10 with chromosomal sfGFP tag; Fm <sup>R</sup>	This work
SGH10::traF	SGH10 with chromosomal integration of <i>traF</i> (from pKPC2) at the Tn7-site downstream of <i>glmS</i>	This work
SGH10ΔwcaJ	Non-capsulated mutant of SGH10 with initial glycosyltransferase gene removed; Fm <sup>R</sup>	2
SGH10ΔrmpA	<i>rmpA</i> deletion mutant of SGH10 with reduced capsular polysaccharide production, leading to decreased hypermucoviscosity and capsule; Fm <sup>R</sup>	This work
SGH10ΔrmpC	<i>rmpC</i> deletion mutant of SGH10 with lower capsule gene expression but do not affect hypermucoviscosity; Fm <sup>R</sup>	This work
SGH10ΔrmpD	<i>rmpD</i> deletion mutant of SGH10 with hypermucoviscosity eliminated without impacting capsule production; Fm <sup>R</sup>	This work
<i>E. coli</i>		
KN02	Nissle 1917 with chromosomal mNeonGreen; Sm <sup>R</sup> Cm <sup>R</sup> (used for all the conjugation experiments, except for tissue imaging)	3
KN02::traF	Nissle KN02 with chromosomal integration of <i>traF</i> (from pKPC2) downstream of <i>glmS</i>	This work
KN03	Nissle 1917; Sm <sup>R</sup> Tc <sup>R</sup> (used only for the gut tissue imaging experiment due to the lack of mNeonGreen)	3
MG1655::Cm <sup>R</sup>	K-12 MG1655; Cm <sup>R</sup>	This work
S17-1 λpir	Conjugation donor carrying an integrated RP4-2 and λpir; Tp <sup>R</sup>	4
HST08	Heat shock Stellar competent cells with high transformation efficiency	TaKaRa Bio
Plasmids	Features	Reference
pKPC2	IncP clinical carbapenemase plasmid; Km <sup>R</sup> (GenBank accession: NZ_MN542377.1)	5
pKPC2-mScarlet3	pKPC2 tagged with mScarlet3; Km <sup>R</sup>	This work
pKPC2ΔtraF	pKPC2 with <i>traF</i> deleted; Km <sup>R</sup>	This work
pNDM1	IncN clinical carbapenemase plasmid; Km <sup>R</sup> (GenBank accession: JADPQD010000004.1)	5
pKpQIL	IncFII clinical carbapenemase plasmid; pKpGFP with Km <sup>R</sup>	This work
RP4-11	IncP plasmid; Km <sup>R</sup> (Addgene # #79812)	6
TP114	IncI plasmid; Km <sup>R</sup> (GenBank accession: MF521836.1)	Institut Pasteur
pOX38	IncFI plasmid; Km <sup>R</sup> (GenBank accession: MF370216.1)	Institut Pasteur
pMNCN064	Environmental IncP clade I plasmid from Japan; Km <sup>R</sup> (GenBank accession: LC623901.1)	7
pYKBP039	Environmental IncP clade I plasmid from Japan; Km <sup>R</sup> (GenBank accession: LC623924.1)	7
pVS0309	Clinical IncP clade II plasmid from Vietnam; Km <sup>R</sup> (GenBank accession: PX308629)	This work
pVS1035	Clinical IncP clade II plasmid from Vietnam; Km <sup>R</sup> (GenBank accession: PX308630)	This work
pR6KTc	Conditional replicative plasmid carrying <i>sacB</i> and <i>oriT</i> ; Tc <sup>R</sup>	2
pACYC184	Low copy number plasmid with a p15A replicon; Cm <sup>R</sup> , Tc <sup>R</sup>	8
pRK2-AraE	IncP plasmid carrying Gm <sup>R</sup> (Addgene #110141)	9
pACYC_traF	Complementation plasmid expressing <i>traF</i> ; Gm <sup>R</sup>	This work
pUC18R6KT-mini-Tn7T-Km	Mini-Tn7 base vector with transcriptional terminator and <i>oriT</i>	10
pJMP1039	Plasmid carrying Tn7 transposases	11

**Supplementary Table 2. List of primers.**

<b>Primer Name</b>	<b>Primer Sequence</b>
pR6K_UP_F	TATGACATGATTACGAATTCCGCTGATAGTTGACCCGGACGGTAAAGGGCTG AACGACCA
pR6K_UP_R	TATCAATTCCCCTATTCTTTATTGCGATAGCCTCATTACTGGCGTCATCATTCTG CAGCAG
pR6K_DOWN_F	AAAGAATAGGGGAATTGATATGGGATTATTTTCATCAGAGTGCGGAGAAGGA GAAGTTAGA
pR6K_DOWN_R	CTTGCATGCCTGCAGGACCGGTTTAGTGCATCCCATGTCATCAAGAATTTCA TCA
pACYC_BB1_F	ACACGGTGCCTGACTGCGTTAGCAATTTAACTGTGATAAA
pACYC_BB1_R	TTTAGCTTCCTTAGCTCCTGAAAATCTCGA
pACYC_BB2_F	TTTTTTTAAGGCAGTTATTGGTGCCCTTAA
pACYC_BB2_R	ATGGAAGCCGCGGCACCTCGCTAACGGATTCACCACTCC
Gm_F	CAGGAGCTAAGGAAGCTAAACCTTTCGGGAGGCCTCTTTTCTGGAATTTGG TACCGAGGA
Gm_R	CAATAACTGCCTTAAAAAAGAATCGGGATATGCAGGCCAAGGCCGCCGCG ATCATCAAG
pUC18R6KT_F	TAGCGGCGGATTTGTCCTAC
pUC18R6KT_R	ATTCCTCGAGAAGCTTGGGC
traFGm_F	GCCCAAGCTTCTCGAGGAATCCTGAAGTCAGCCCCATAC
traFGm_R	GTAGGACAAATCCGCCGCTACTGAACAGGAGGGACAGC

## Supplementary References

- 1 Lam, M. M. C. *et al.* Population genomics of hypervirulent *Klebsiella pneumoniae* clonal-group 23 reveals early emergence and rapid global dissemination. *Nat Commun* **9**, 2703, doi:10.1038/s41467-018-05114-7 (2018).
- 2 Tan, Y. H., Chen, Y., Chu, W. H. W., Sham, L. T. & Gan, Y. H. Cell envelope defects of different capsule-null mutants in K1 hypervirulent *Klebsiella pneumoniae* can affect bacterial pathogenesis. *Mol Microbiol* **113**, 889-905, doi:10.1111/mmi.14447 (2020).
- 3 Neil, K., Allard, N., Grenier, F., Burrus, V. & Rodrigue, S. Highly efficient gene transfer in the mouse gut microbiota is enabled by the Incl(2) conjugative plasmid TP114. *Commun Biol* **3**, 523, doi:10.1038/s42003-020-01253-0 (2020).
- 4 de Lorenzo, V., Cases, I., Herrero, M. & Timmis, K. N. Early and late responses of TOL promoters to pathway inducers: identification of postexponential promoters in *Pseudomonas putida* with lacZ-tet bicistronic reporters. *J Bacteriol* **175**, 6902-6907, doi:10.1128/jb.175.21.6902-6907.1993 (1993).
- 5 Yong, M. *et al.* Dominant Carbapenemase-Encoding Plasmids in Clinical Enterobacterales Isolates and Hypervirulent *Klebsiella pneumoniae*, Singapore. *Emerg Infect Dis* **28**, 1578-1588, doi:10.3201/eid2808.212542 (2022).
- 6 Quandt, J. *et al.* Modified RP4 and Tn5-Mob derivatives for facilitated manipulation of large plasmids in Gram-negative bacteria. *Plasmid* **52**, 1-12, doi:10.1016/j.plasmid.2004.04.002 (2004).
- 7 Hayakawa, M. *et al.* Hitherto-Unnoticed Self-Transmissible Plasmids Widely Distributed among Different Environments in Japan. *Appl Environ Microbiol* **88**, e0111422, doi:10.1128/aem.01114-22 (2022).
- 8 Chang, A. C. & Cohen, S. N. Construction and characterization of amplifiable multicopy DNA cloning vehicles derived from the P15A cryptic miniplasmid. *J Bacteriol* **134**, 1141-1156, doi:10.1128/jb.134.3.1141-1156.1978 (1978).
- 9 Cook, T. B. *et al.* Genetic tools for reliable gene expression and recombineering in *Pseudomonas putida*. *J Ind Microbiol Biotechnol* **45**, 517-527, doi:10.1007/s10295-017-2001-5 (2018).
- 10 Choi, K. H. *et al.* A Tn7-based broad-range bacterial cloning and expression system. *Nat Methods* **2**, 443-448, doi:10.1038/nmeth765 (2005).
- 11 Peters, J. M. *et al.* Enabling genetic analysis of diverse bacteria with Mobile-CRISPRi. *Nat Microbiol* **4**, 244-250, doi:10.1038/s41564-018-0327-z (2019).